

## ORIGINAL ARTICLE

# Rheological Investigation of a Set of PCE Superplasticizers in Cement

Thomas Wagner<sup>1</sup> | Torben Gädt<sup>1</sup>

## Correspondence

Prof. Dr. Torben Gädt  
Technical University of Munich  
TUM School of Natural Sciences  
Department of Chemistry  
Chemistry of Construction Materials  
Lichtenbergstr. 4  
85748 Garching b. München  
Email: [torben.gaedt@tum.de](mailto:torben.gaedt@tum.de)

<sup>1</sup> Technical University of Munich,  
Garching, Germany

## Abstract

The importance of polycarboxylate ethers (PCE) as concrete superplasticizers has significantly increased in recent decades, both technically and commercially. At the least, three descriptors describe the average PCE structure: the side chain length (P), the charge density (N), and the number of repeating units (n). The synthesis parameters determine the average composition of the PCEs and, consequently, their performance in cementitious materials. This study examines the rheological properties of 27 different PCE structures, which were synthesized using redox-initiated free-radical copolymerization. We independently varied the parameters P and N and produced three PCEs with different molar weights for each combination of P and N. Cement pastes with low PCE dosages of 0.035 wt% were tested in a rheometer using a plate-plate geometry. It turns out that when the PCE is added directly to the mixing water, the PCE has a complex influence on the very early hydration. Consequently, the obtained rheology data is not entirely in line with available structure-activity relationships. Additionally, we attempted to model the observed rheology data based on three structural PCE descriptors. While a multivariate linear regression model failed to accurately describe the relationship, a random forest model delivered a better model. In summary, we conclude that the impact of PCEs on early hydration significantly affects the rheology of the paste. The changed hydration pathway causes a deviation of our results from existing structure-activity relationships and makes it challenging to statistically model the sparse rheology data with a minimal set of three structural descriptors.

## Keywords

Superplasticizer, PCE, Rheology, Synthesis, Machine Learning, Cement, Cement Hydration

## 1 Introduction

Polycarboxylate ethers (PCE) are the most important superplasticizer class [1]. Their structure affects the dosage needed to obtain a desired dispersion at a defined w/c value and also influences the early strength by retarding the cement hydration [2]. PCE are synthesized by free-radical polymerization and generally consist of polyethylene glycol (PEG) side chains attached to a negatively charged backbone of carboxylate monomers, as shown in Figure 1. Their structure is described as follows: the number of repeating units in a side chain, i. e. its length, is denoted as P. The letter N describes the number of monomers per polymer repeat unit. The parameter n describes the number of repeating units in a polymer. Note that a repeat unit comprises the side chain monomer and (N-1) charge-carrying monomers.

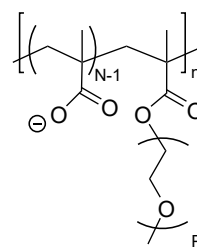


**Figure 1** Structure of a methacrylate-based PCE. A PCE with only one type of side chain carrying monomer has (N-1) charged monomers for each side chain monomer.

The molecular weight of the macromonomer determines P. Finally, the CTA amount and the initiator concentration influence the backbone length n. The chemical structure analysis of the obtained PCE can be challenging [3,4]. Gel permeation chromatography (GPC) gives insight into the molar mass distribution of the resulting PCE molecules but does not provide information about the monomer distribution within the polymer chains.

During GPC analysis, for example, PCE molecules with longer backbone length  $n$  can be eluted in the same weight fraction as shorter ones with a higher side chain density. Since the synthesis conditions and raw material chemistry determine the characteristics of a PCE, we set out to examine the relationship between the synthesis parameters and the rheological properties of cement pastes containing the PCE.

The effectivity of PCEs to lower the yield stress of a cement paste depends on their ability to adsorb onto clinker and hydrate surfaces [5,6]. The side chains establish steric repulsion among the covered particles [7]. Winnefeld et al. describe larger dosage efficiency for lower side chain densities [6]. Higher adsorption rates were reported to correlate with stronger dispersion abilities of the PCEs [8]. The affinity of a PCE for cementitious surfaces drives the adsorption and is generally large for high charge densities and short side chains. On the other hand, large side chain densities (small  $N$  values) or long side chains (large  $P$ ) reduce the adsorption affinity of the PCE [6,9]. The relationship between the adsorption constant of a PCE and its structure was described by Marchon et al. [8] by equation (1).

$$K_A \approx \frac{z^2(N-1)^2}{nP^{9/5}N^{3/5}} \quad (1)$$

Here,  $z$  is the charge number of the charged monomer ( $z=1$  in the case of methacrylic acid). The inverse value of  $K_A$  is the desorption constant  $K_A^{-1}$ . A large desorption constant corresponds to a PCE with a low surface affinity. The desorption constant increases with  $P/N$  (Figure 2). Furthermore, the slump flow diameter  $D$  for a specific polymer dosage  $c$  was formulated by Marchon et al. [2] as a function of  $P$  and  $N$  (see equation (2)).

$$c = \frac{D - D_0}{0.76\gamma_1} \left(\frac{N}{P}\right)^{\gamma_2} \quad (2)$$

For the empirically determined constants  $\gamma_1$  and  $\gamma_2$ , the suggested values of 237 and 0.17 were chosen [2].  $D_0$  is the diameter of the cone used in the slump flow test. The yield stress  $\tau_0$  is calculated from the radius  $R$  of the slump flow by equation (3) [10]

$$\tau_0 = \frac{225\rho gV^2}{128\pi^2 R^5} \quad (3)$$

where  $\rho$  is the density of the cement paste,  $g$  is the standard gravity, and  $V$  is the volume of the cone. According to the model of Marchon (equation (2)), at a given dosage, the slump flow  $D$  is proportional to the ratio of  $P/N$  to the power of an empirically determined constant. Equation (3) and equation (2) can be combined to provide a relation between the yield stress and  $P/N$  (equations (4)–(7)). The yield stress decreases monotonically with  $P/N$  (red curve in Figure 2).

$$D = 0.76\gamma_1 c \left(\frac{P}{N}\right)^{\gamma_2} + D_0 \quad (4)$$

$$D = 2R \quad (5)$$

$$R = \frac{0.76}{2}\gamma_1 c \left(\frac{P}{N}\right)^{\gamma_2} + R_0 \quad (6)$$

$$\tau_0 = \frac{225\rho gV^2}{128\pi^2} \left(\frac{0.76}{2}\gamma_1 c \left(\frac{P}{N}\right)^{\gamma_2} + R_0\right)^{-5} \quad (7)$$

This model implies that long side chains (i. e., large  $P$  values) and low charge densities (i. e., low  $N$  values) lead to low yield stresses. However, the model does not account for a reduced adsorption constant of PCEs with large  $P/N$  ratios. Another limitation of the model is related to the dosage mode of the PCE: equation (2) was derived from slump flow data of cement pastes with delayed addition of the PCEs. Note that this differs from the findings of Winnefeld and Zingg, who added PCEs with the mixing water and reported larger dosage efficiencies for lower side chain densities [6,11], i. e., larger  $N$  or smaller  $P/N$  ratios.

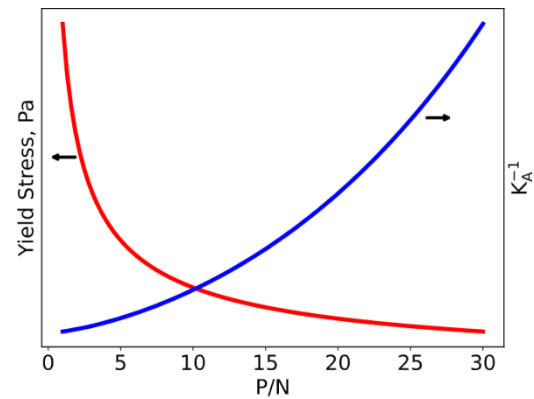


**Figure 2** Theoretical dependence of the yield stress (red curve) and the desorption constant  $K_A^{-1}$  (blue curve) on  $P/N$ , derived from Marchon [8,12]. In red: yield stress calculated for a  $w/c$  of 0.38 and a polymer dosage of 0.035 %bwoc (equation (7)). In blue: desorption constant calculated for a constant value of  $P=113$  and  $n=15$  (equation (1)). The relative scaling of the y-axes is arbitrary. Therefore, the intersection of both curves is also arbitrary. The plot serves to demonstrate the expected convex curvature for the dependence of the yield stress on  $P/N$ .

Figure 2 suggests that the yield stress decreases for increasing values of  $P/N$ , and the desorption constant  $K_A^{-1}$  increases with  $P/N$ . The yield stress relation does not consider the reduced surface affinity at large  $P/N$  values, which will lead to increasing amounts of desorbed PCE. Therefore, although the exact functional relationship is unknown, the yield stress dependency on  $P/N$  will have a convex curvature.

PCEs have a strong influence on the cement hydration, including the amount and particle size distribution of forming hydration products, which consequently affects the rheological properties of the paste [2,13,14]. The early reactivity of the cement determines the rheology of the paste, and is governed in large part by the dissolution of  $C_3A$  and the precipitation of ettringite [15]. Jakob et al. have shown that the early ettringite formation is a major influence on the rheology of the cement paste [16]. During the growth of ettringite, water from the pore solution is consumed, which leads to a higher solid volume fraction,

and thus, the yield stress increases according to the YODEL model [17]. Direct addition of the PCE with the mixing water strongly modifies the early  $C_3A$  reaction of the cement [12,13,18–23]. Three distinct effects can be discerned: First, Stroh et al. found that the amount of ettringite during the first 20 minutes is enhanced in the presence of highly charged PCE [21]. The enhanced formation of ettringite leads to a higher yield stress of the paste due to changes in the solid volume fraction and the surface area. Second, the site of ettringite nucleation is shifted from the surface of  $C_3A$  to the pore solution of the cement paste [14,24]. And third, PCEs hinder the growth of individual ettringite crystals, which then undergo elongation [25]. Larger effects were found for higher charged PCEs. While individual crystals are hindered in their growth, the total amount of formed ettringite is increased. Consequently, smaller crystals are formed which possess a higher specific surface area than in the case without PCE [18,26]. The formation of additional surface area further consumes free PCE, which is hence no longer available for the dispersion of other particles. In summary, PCEs which possess a high charge density were found to have a stronger impact on the early hydration of cement, which includes changes in the amount, the formation site, and the morphology of ettringite. These changes lead to a larger surface area content of the formed ettringite, which drastically affects the rheology of the paste.

While the structure-activity relationship of PCEs is well-established for delayed addition, knowledge is more limited if they are added to the mixing water. Despite the aforementioned relationships, a comprehensive picture of the precise interactions of the PCEs with the initial hydration process and the resulting rheological properties of the paste is still missing.

This study aims to provide data on the effects of various PCE structures on the early rheology of cement paste. Therefore, we synthesized a set of 27 PCEs by varying the parameters: P, N, and n. Here, the amounts of CTA and initiator control n, while the monomer choice and monomer ratio determine P and N. The yield stress of cement pastes containing a PCE dosage of 0.035 %bwoc (by weight of cement) was measured using a rotational rheometer. We compare the resulting data with existing structure-activity relationships and test multivariate linear regression and random forest models.

## 2 Experimental

### 2.1 Material

The polyethyleneglycol methacrylates, methacrylic acid (MAA, stabilized with hydroquinone monomethyl ether), 3-mercaptopropionic acid (3-MPA), tert-butyl hydroperoxide (tBHP), and sodium formaldehyde sulfoxylate dihydrate (SFS) were obtained from commercial suppliers and used as received. A commercial CEM I 42.5 R ordinary Portland cement was used in this study.

### 2.2 Synthesis

PCEs were synthesized in small-scale reactions with a volume of 10 mL. An aqueous solution of macromonomer and

MAA was prepared and weighed into small vials for each combination of P and N. To the stirred monomer solutions varying amounts of 3-MPA (CTA agent), SFS (1.1 times the respective molar amount of tBHP), and tBHP (initiator, 0.6 - 3 mol% to the total amount of monomers) were added at 25 °C. For instance, the PCE with the parameters P=23, N=5.2, and a CTA dosage of 2 mol% was synthesized by adding a solution of 3-MPA (0.564 mL, 32 mg, 0.3 mmol), a solution of SFS (0.941 mL, 47 mg, 0.3 mmol), water (0.49 mL), and a solution of tBHP (0.941 mL, 27 mg, 0.3 mmol) to a mixture of polyethyleneglycol methacrylate (P=23, 3.1 g, 3 mmol) and MAA (1.0 g, 12 mmol) containing 3.5 mL water from the macromonomer. The reaction mixture was stirred for two hours and was analyzed by GPC and  $^1H$  NMR. The synthesis parameters are shown in Figure 3. N was chosen to include some unconventional P/N ratios. Therefore, the set contains low values for P/N (e. g., around 2), especially for PCEs with short side chains (P=23). The PDIs of most polymers are between 1.6 and 2.0. However, for one macromonomer (P=45), we obtained PDI values between 2 and 3, which is unusually broad and is most likely related to a lower raw material quality for this macromonomer (this was not checked in detail, however).

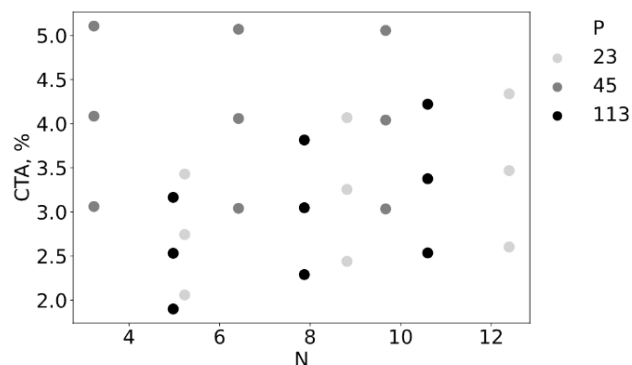


**Figure 3** Variations of the synthesis parameter. For each value of P, PCEs were prepared at three values for N, and three different amounts of CTA (in mol% to the total amount of monomers present in the reaction).

### 2.3 Rheometry

In a typical experiment, 40 g cement were added to a solution of PCE in water at a water/cement ratio (w/c) of 0.36 and a dosage of 0.035 %bwoc of the PCE. The paste was stirred with a four-blade mixer (IKA Eurostar 20) at 600 rpm for one minute, followed by a one-minute rest time, and remixed at the same speed for another minute. The paste rested for 10 minutes, was stirred once more for one minute, and then used for the rheometer experiment (Anton Paar, serrated plates (diameter = 25 mm), gap width of 1 mm). The measurement program started 20 minutes after the cement came in contact with water. It included 10 seconds of a pre-shear phase at  $80 \text{ s}^{-1}$ , followed by a stepwise descending shear rate  $\dot{\gamma}$  starting at  $80 \text{ s}^{-1}$  and arriving at  $0.01 \text{ s}^{-1}$  within 14 steps. The range within 60 to  $20 \text{ s}^{-1}$  was considered for evaluating the yield stress  $\tau_0$  and the viscosity  $\eta$  according to the Bingham equation (8).

$$\tau = \tau_0 + \eta \cdot \dot{\gamma} \quad (8)$$

## 2.4 Machine Learning Models

A multivariate linear regression model and a random forest regression model were implemented in Python using the scikit-learn package [27]. The random forest regression model operates on an estimator number (number of trees) of 100 at a varying depth until all nodes are expanded to pure leaves. The trees are created based on bootstrapped datasets. The data set was randomly split into a training set (70% of the experiments) and a testing set (30%). Three polymer parameters were used to predict the yield stress: 1) the carboxylate dosage per gram cement, i. e., the content of carboxylate groups that are dosed to one gram cement, 2) P/N, and 3) the CTA dosage in mol% employed during synthesis. The carboxylate dosage is given in mol carboxylate groups per gram of cement and is calculated based on the molar mass of the repeating unit by equation (9).

$$\text{Carboxylate Dosage} = \frac{0.035\%bwoc}{M_{\text{repeating unit}}} \cdot (N - 1) \quad (9)$$

## 3 Results and Discussion

### 3.1 Experimental Results

A set of PCEs with varying structural parameters (P, N) and varying synthesis parameters (CTA and initiator content) was synthesized. Each polymer was added to the mixing water, and cement pastes ( $w/c = 0.36$ ) were prepared with a constant PCE dosage (0.035%, weight polymer by weight cement). The dynamic yield stress was determined by fitting a Bingham model to the  $\tau, \dot{\gamma}$ -curve of the paste between 20 and 60  $s^{-1}$ .

The measured yield stress is shown in Figure 4 as a function of the ratio of P/N. Three vertically stacked points are found for each P/N ratio due to different values of n. Notably, the P/N values for P=23 are small compared to conventional PCE, i. e., they correspond to very highly charged PCE.

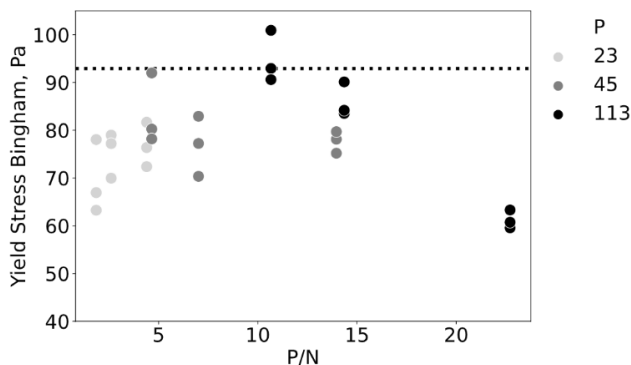


**Figure 4** Yield stress values as a function of P/N. The dashed line marks the yield stress of the cement paste without PCE. Each value for P/N contains three polymers with different n, which were synthesized with varying amounts of CTA.

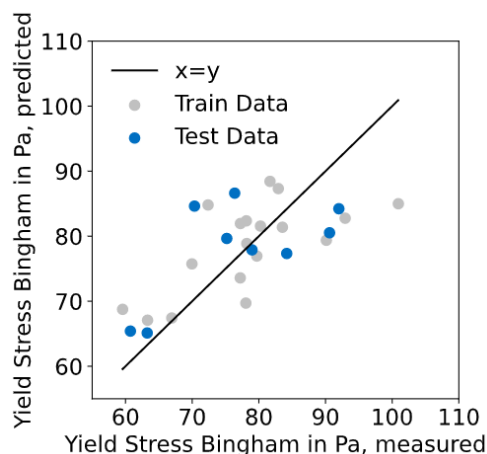
The experimental distribution of their yield stress  $\tau$  against P/N shows a concave curvature, contrasting what we expected from structural considerations as discussed earlier (see Figure 2)).

Some PCEs increase the yield stress beyond the value for blank cement paste, suggesting that their impact on the hydration process, which compromises workability, exceeds their inherent dispersing ability. Based on reported results, higher charge densities of the PCE are expected to increase the reactivity in the first minutes [21]. The increased formation of ettringite particles with higher surface content would increase the yield stress. However, the lowest yield stress values were achieved with the highest and lowest values of P/N, respectively. Surprisingly, the highest charge density, i. e., the lowest P/N ratio, results in low yield stresses comparable to large P/N values (black points with  $P/N > 20$ ). As discussed above, increasing P/N values should lead to decreasing yield stresses and decreasing surface affinities of the PCE. A third parameter influenced by the P/N ratio is the formation of ettringite and the reactivity of the  $C_3A$  phase. If the PCE is added to the mixing water, the influence of PCE on the  $C_3A$  reactivity dominates their behavior. Further studies are ongoing to improve the understanding of the influence of the PCE structure on the early hydration.

### 3.2 Machine Learning Models

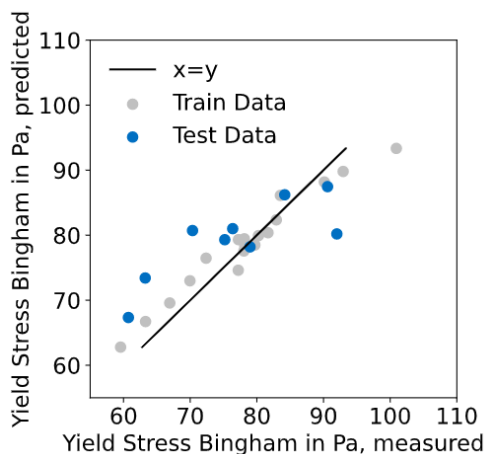
We built a simple multivariate linear regression and a random forest model to the Bingham yield stress using three predictor variables: the carboxylate dosage per cement ( $\mu\text{mol g}^{-1}$ ), P/N, and the amount of CTA used during synthesis. Both models were trained on a subset of 70% of the data set's experiments (18 data points).

Figure 5 shows the predicted Bingham yield stress of the multivariate linear regression model for the training and the test data. The coefficient of determination  $R^2$  of the predicted training data, which the model had not seen before, is 0.431, and a root mean squared error of 7.92 Pa was determined. The simple linear model with three parameters fails to predict the yield stress reliably.



**Figure 5** Measured yield stress values and predicted values based on a multivariate linear regression with the predictor variables carboxylate dosage, P/N, and CTA content. The black line indicates perfect prediction.

The random forest model is another regression model suitable for small data sets. We use the same variables and data splitting to model the yield stress. The predicted values of the random forest model are plotted against the measured values in Figure 6.



**Figure 6** Measured yield stress values and predicted values based on a random forest model with the predictor variables carboxylate dosage, P/N, and CTA content. The black line indicates perfect prediction.

The prediction of the test data set, which the model had not seen before, shows a coefficient of determination  $R^2 = 0.66$  and a root mean squared error of 7.05 Pa. The predictions are closer to the experimental values than those obtained from the multivariate linear regression model. We use the obtained model to predict the yield stress (Figure 7) as a function of P/N for a fixed CTA dosage of 4 mol% and a fixed carboxylate dosage of  $1 \mu\text{mol g}^{-1}$ . The carboxylate dosage corresponds to the amount of introduced carboxylate groups per gram of cement and represents an average value across the samples. Due to the underlying calculation (equation (9)), the carboxylate dosage and P/N are not independent.

The linear regression model produces a linearly declining yield stress, and the random forest model yields a prediction profile similar to the original data, i. e., predicting the highest yield stress values for medium values of P/N.

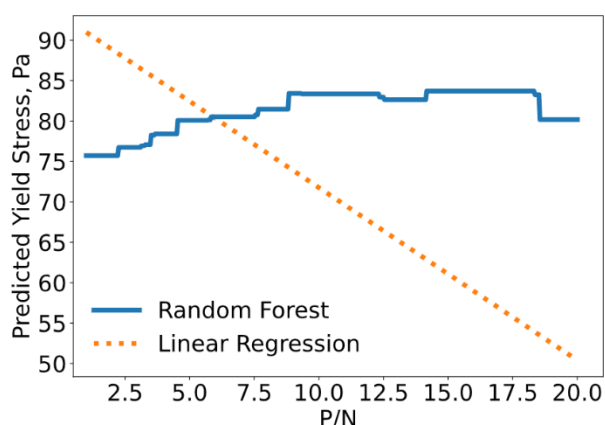


**Figure 7** Prediction profiles of the models for different P/N values at constant values for the carboxylate dosage ( $1 \mu\text{mol g}^{-1}$ ) and a CTA dosage of 4 mol%.

### 3.3 Limitations

While this study offers valuable insights, we want to highlight some limitations. First, the range of PCE structures comprises some unusual cases. Notably, the PCEs with  $P=23$  represent very high charge densities. Second, the dataset exclusively consists of methacrylic PCEs synthesized via one specific route. Third, this study does not contain a mechanistic investigation of the observed patterns, especially concerning the influence of the PCE on the early hydration. Fourth, the explored data set is small for statistical modeling purposes. Therefore, considering a more extensive set of predictor variables is impossible.

## 4 Conclusions

In this study, we have synthesized 27 different PCEs and determined the yield stress of cement pastes at a w/c ratio of 0.36 and a PCE dosage of 0.035%. Based on theoretical considerations, we expected to find a convex distribution of the yield stress values as a function of P/N, with the lowest yield stress for intermediate values of P/N. However, we found a concave distribution. The lowest yield stress values were found for high and low values for P/N, respectively. We explain this by assuming that PCEs added to the mixing water strongly affect the hydration processes of the cement paste. The formation of increasing amounts of initial ettringite leads to a decrease of the effective w/c value due to the incorporation of water and, more importantly, significantly increases the total surface area of the suspension at early ages. Surprisingly, small P/N values lead to decreased yield stress. It is, therefore, essential to quantitatively describe the effect of PCE on the early hydration of the cement and the formation of ettringite for the considered P/N ratios. Such a study is an objective for future work.

The machine learning models were of low to modest quality. A more comprehensive structural description of the PCE would provide sufficient information to predict their rheological properties accurately. For our case, it can therefore be concluded that essential information on PCE chemistry is still missing in the data. As the available dataset for training contained less than 20 experiments, it was not possible to include all available synthesis parameters due to the risk of overfitting. Subsequent datasets should ideally contain a significantly increased number of experiments and a narrower distribution of PCE structure parameters.

## References

- [1] Lei, L.; Hirata, T.; Plank, J. (2022) *40 years of PCE superplasticizers - History, current state-of-the-art and an outlook*. Cem. Concr. Res., 157, p. 106826. <https://doi.org/10.1016/j.cemconres.2022.106826>
- [2] Marchon, D.; Boscaro, F.; Flatt, R. J. (2019) *First steps to the molecular structure optimization of polycarboxylate ether superplasticizers: Mastering fluidity and retardation*. Cem. Concr. Res., 115, pp. 116–123. <https://doi.org/10.1016/j.cemconres.2018.10.009>
- [3] Gelardi, G. (2017) *Characterization of Comb Copolymer Superplasticizers by a Multi-Technique Approach* [Dissertation]. ETH Zurich.
- [4] Weckwerth, S. A.; Radke, W.; Flatt, R. J. (2021) *A Method for Characterizing the Chemical Heterogeneity of Comb-Copolymers and Its Dependence on Synthesis Routes*. Polymers, 13 (12). <https://doi.org/10.3390/polym13121921>
- [5] Mollah, M. Y. A. et al. (2000) *A review of cement-superplasticizer interactions and their models*. Adv. Cem. Res., 12 (4), pp. 153–161. <https://doi.org/10.1680/adcr.2000.12.4.153>.
- [6] Winnefeld, F. et al. (2007) *Effects of the molecular architecture of comb-shaped superplasticizers on their performance in cementitious systems*. Cem. Concr. Compos., 29 (4), pp. 251–262. <https://doi.org/10.1016/j.cemconcomp.2006.12.006>
- [7] Uchikawa, H.; Hanehara, S.; Sawaki, D. (1997) *The role of steric repulsive force in the dispersion of cement particles in fresh paste prepared with organic admixture*. Cem. Concr. Res., 27 (1), pp. 37–50. [https://doi.org/10.1016/S0008-8846\(96\)00207-4](https://doi.org/10.1016/S0008-8846(96)00207-4)
- [8] Marchon, D. et al. (2013) *Molecular design of comb-shaped polycarboxylate dispersants for environmentally friendly concrete*. Soft matter, 9 (45), p. 10719. <https://doi.org/10.1039/C3SM51030A>
- [9] Weckwerth, S. A.; Temme, R. L.; Flatt, R. J. (2022) *Experimental method and thermodynamic model for competitive adsorption between polycarboxylate comb copolymers*. Cem. Concr. Res., 151, p. 106523. <https://doi.org/10.1016/j.cemconres.2021.106523>
- [10] Roussel, N.; Coussot, P. (2005) *"Fifty-cent rheometer" for yield stress measurements: From slump to spreading flow*. J. Rheol., 49 (3), pp. 705–718. <https://doi.org/10.1122/1.1879041>
- [11] Zingg, A. et al. (2009) *Interaction of polycarboxylate-based superplasticizers with cements containing different C3A amounts*. Cem. Concr. Compos., 31 (3), pp. 153–162. <https://doi.org/10.1016/j.cemconcomp.2009.01.005>
- [12] Marchon, D.; Flatt, R. J. (2016) *Impact of chemical admixtures on cement hydration* in: Aïtcin, P.-C., Flatt, R. J. [Eds.]. Science and Technology of Concrete Admixtures. Cambridge: Elsevier Ltd., pp. 279–304.
- [13] Zingg, A. et al. (2008) *Adsorption of polyelectrolytes and its influence on the rheology, zeta potential, and microstructure of various cement and hydrate phases*. J. Colloid Interface Sci., 323 (2), pp. 301–312. <https://doi.org/10.1016/j.jcis.2008.04.052>
- [14] Zingg, A. et al. (2008) *The microstructure of dispersed and non-dispersed fresh cement pastes – New insight by cryo-microscopy*. Cem. Concr. Res., 38 (4), pp. 522–529. <https://doi.org/10.1016/j.cemconres.2007.11.007>
- [15] Jansen, D. et al. (2018) *The early hydration of OPC investigated by in-situ XRD, heat flow calorimetry, pore water analysis and 1H NMR: Learning about adsorbed ions from a complete mass balance approach*. Cem. Concr. Res., 109, pp. 230–242. <https://doi.org/10.1016/j.cemconres.2018.04.017>
- [16] Jakob, C. et al. (2019) *Relating Ettringite Formation and Rheological Changes during the Initial Cement Hydration: A Comparative Study Applying XRD Analysis, Rheological Measurements and Modeling*. Materials (Basel, Switzerland), 12 (18). <https://doi.org/10.3390/ma12182957>
- [17] Flatt, R. J.; Bowen, P. (2006) *Yodel: A Yield Stress Model for Suspensions*. J. Am. Ceram. Soc., 89 (4), pp. 1244–1256. <https://doi.org/10.1111/j.1551-2916.2005.00888.x>
- [18] Dalas, F. et al. (2015) *Modification of the rate of formation and surface area of ettringite by polycarboxylate ether superplasticizers during early C3A–CaSO4 hydration*. Cem. Concr. Res., 69, pp. 105–113. <https://doi.org/10.1016/j.cemconres.2014.12.007>
- [19] Marchon, D. et al. (2017) *Molecular and submolecular scale effects of comb-copolymers on tri-calcium silicate reactivity: Toward molecular design*. J. Am. Ceram. Soc., 100 (3), pp. 817–841. <https://doi.org/10.1111/jace.14695>
- [20] Wang, X. et al. (2022) *Compatibility between Polycarboxylate Ether with Different Charge Densities and Cement*. J. Mater. Civ. Eng., 34 (1). [https://doi.org/10.1061/\(ASCE\)MT.1943-5533.0004035](https://doi.org/10.1061/(ASCE)MT.1943-5533.0004035)
- [21] Stroh, J. et al. (2016) *Time-resolved in situ investigation of Portland cement hydration influenced by chemical admixtures*. Constr. Build. Mater., 106, pp. 18–26. <https://doi.org/10.1016/j.conbuildmat.2015.12.097>
- [22] Shi, C. et al. (2016) *Effects of superplasticizers on the stability and morphology of ettringite*. Constr. Build. Mater., 112, pp. 261–266. <https://doi.org/10.1016/j.conbuildmat.2016.02.198>

- [23] Pott, U. et al. (2020) *Investigation of the Early Cement Hydration with a New Penetration Test, Rheometry and In-Situ XRD* in: Mechtcherine, V., Khayat, K., Secieru, E. [Eds.]. *Rheology and Processing of Construction Materials – RheoCon2 & SCC9*. Vol. 23. Cham: Springer International Publishing, pp. 246–255.
- [24] Winnefeld, F. et al. (2009) *The ettringite – superplasticizer interaction and its impact on the ettringite distribution in cement suspensions*. Ninth ACI International Conference on Superplasticizers and Other Chemical Admixtures. Gupta, P., Holland, T. C., Malhotra, V. M. [Eds.], Seville, Spain, 2009. Farmington Hills, Mich.: American Concrete Inst.
- [25] Sha, S. et al. (2022) *Effect of polycarboxylate superplasticizers on the growth of ettringite in deionized water and synthetic cement pore solution*. *Constr. Build. Mater.*, 341, pp. 127602. <https://doi.org/10.1016/j.conbuildmat.2022.127602>
- [26] Yamada, K. (2009) *A Summary of Important Characteristics of Cement and Superplasticizers*. Ninth ACI International Conference on Superplasticizers and Other Chemical Admixtures. Gupta, P., Holland, T. C., Malhotra, V. M. [Eds.], Seville, Spain, 2009. Farmington Hills, Mich.: American Concrete Inst.
- [27] Pedregosa, F. et al. (2011) *Scikit-learn: Machine Learning in Python*. *JMLR*, 12 (85), pp. 2825–2830.